CONF-840520--19

UCRL- 90160
PREPRINT

PLASMA-SURFACE INTERACTIONS IN LARGE TANDEM MIRROR DEVICES--MFTF-B

S. L. Allen and the
TMX-U/MFTF-B Experimental Team

This report was prepared for submittal to the 6th International Conference on Plasma Surface Interactions in Fusion Devices, Nagoya, Japan, May 14-18, 1984.

May 7, 1984

Lawrence Livermore National Laboratory

DISCLAIMER

PLASMA-SURFACE INTERACTIONS IN LARGE TANDEM MIRROR DEVICES--MFTF-B*

S. L. Allen and the TMX-U/MFTF-B Experimental Team
Lawrence Livermore National Laboratory, University of California
Livermore, CA 94550

UCRL--90160
DE85 001753

ABSTRACT

Present experiments on TMX-U and modeling of MFTF-B indicate that plasma-surface interactions can be controlled in MFTF-B. The MFTF-B configuration uses a hot electron population created by ECRH and a sloshing-ion population created by neutral beams in the thermal barrier region to create a potential that confines the central cell ions. Neutral beams and ICRH are used to heat the central cell ions. Plasma-surface interactions can be minimized at radial surfaces by control of the axial confinement of the edge plasma. The thermal barrier configuration is sensitive to the background neutral density, and requires low wall reflux and efficient shielding by the edge plasma. Glow discharge cleaning, titanium gettering, and control of the gas from neutral beams will be used to provide wall conditioning and to reduce the background gas pressure. The shielding efficiency of the plasma edge has been modeled in MFTF-B by comparing computer codes with current experimental measurements. In addition, it is very important to reduce high-energy neutral-beam-injected impurities; this is accomplished by using gettering or magnetic separation

in the injector systems. Plasma-edge scrapers, diverter-like devices, and direct-conversion equipment will be located in the end region. Major disruptions are not anticipated. Finally, MFTF-B will also test some technological issues that are revelant to reactors: superconducting magnet systems and nearly steady-state (30-s) operation.

*Work performed under the auspices of the U.S. Department of Energy by the Lawrence Livermore National Laboratory under contract number W-7405-ENG-48.

1. INTRODUCTION

Plasma-surface interactions can play an important role in the present generation of tandem mirror machines, such as the Tandem Mirror Experiment-Upgrade (TMX-U) [1], Phaedrus [2], and Gamma-10 [3], which are currently operational, and AMBAL [4] and TARA [5], which will soon be fully operational. The importance of plasma-surface interactions may be even more pronounced in larger, longer-pulse tandem mirrors used to investigate plasmas at reactor-like conditions. However, current experiments and models of future experiments indicate that plasma-surface interactions can be minimized in tandem mirror machines. This is due to the inherent open field lines of the confinement configuration. In particular, plasma-surface interactions can be controlled at radial surfaces by controlling the axial confinement of the edge plasma.

The Mirror Fusion Test Facility (MFTF-B), which is under construction at the Lawrence Livermore National Laboratory (LLNL), is an example of the next generation of large (64-m axial length), long-pulse (30-s) machines. We present here a description of MFTF-B, with emphasis on the issues concerned with plasma-surface interactions. A qualitative discussion of the thermal barrier mode of axial confinement is presented in Sec. 2. The thermal barrier is an integral part of a tandem mirror, and it dictates the required plasma conditions particularly at the plasma-surface. The experimental configuration used in MFTF-B to create the thermal barrier is then examined in detail in Sec. 3. In Sec. 4 the relevant plasma-surface interaction issues are addressed, and in several cases experimental results from currently operating tandem mirror machines are included because they serve as a guide for the design and operation of MFTF-B. Section 5 is a summary and a discussion of future work concerned with plasma-surface interactions in tandem mirrors.

Several issues are outside the scope of the present paper and are presented elsewhere. Reference 6 contains a detailed examination of experiments concerned with plasma-surface interactions in TMX and TMX-U. Reference 7 describes several upgrades to MFTF, including steady-state (100-hour) operation with DT fuel and the creation of a region of very high neutron flux (2 MW/m^2) to test various blanket designs. Issues relevant to tandem mirror reactor designs such as MARS are discussed in Ref. 8.

2. THE THERMAL BARRIER PLASMA ENVIRONMENT

To understand the importance of the function of a thermal barrier mode in a tandem mirror, and in turn to appreciate the requirements it places on the plasma-surface interactions, it is necessary to briefly trace the evolution of mirror experiments. Along each step of the development, modifications have been motivated by the need for an efficient reactor concept.

The early single-mirror experiments showed that to control magnetohydrodynamic (MHD) stability, the plasma sould be confined in a magnetic well, or "minimum-B" configuration [9]. This requirement motivated the design of highly efficient magnetic geometries, such as the yin-yang quadrupole [10], which also have good access for neutral beam injection. Similar magnet designs are used in modern day mirror devices including MFTF-B.

The next set of experiments was concerned with the effect of high-frequency modes (on the order of the ion gyrofrequency) on a mirror plasma with neutral beam injection. These modes [such as the drift cyclotron loss cone (DCLC)] are driven by the non-Maxwellian velocity distributions present in mirror plasmas [11]. These modes cause diffusion in velocity space and can thereby increase plasma losses significantly. Several experiments, including 2XIIB, showed that the DCLC mode could be stabilized by introducing a low-energy plasma stream [12]. This was a major breakthough in mirror physics; however, it was also soon realized that a reactor based on a single mirror involved a large amount of circulating power. The expected Q (the ratio of fusion power produced to injected power) from such a reactor was on the order of unity because Coulomb scattering losses imposed a fundamental limit on plasma confinement [13].

The tandem mirror was invented to overcome the reactor limitations of a single mirror, while incorporating its inherent advantages. The tandem mirror is composed of two mimimum-B mirror cells (end plugs) with high energy neutral beam injection; these are located at each end of a straight solenoidal section (central cell). The end plugs provide the MHD stablility for the system, and the central cell plasma furnishes the required lower energy ions for microstability. This configuration adds another dimension to confinement: if the end cell plasma is more dense than the central cell, an axial ambipolar potential is established which confines the ions in the central cell. Experiments on TMX showed that the confinement time in a tandem mirror machine could be increased at least an order of magnitude compared with a single mirror [14]. The plasma was also nearly microstable, exhibiting only low level fluctuations attributed mostly to the Alfven ion cyclotron (AIC) mode [15].

In its early form, however, tandem mirror reactor designs required high end plug magnetic fields and a high beam injection energy. This is because the ion confining potential is established by the density difference between the central cell and the end plug; it scales logarithmically with density: $\phi = T_e \ln(n_p/n_c)$. On the other hand, the ratio of central cell fusion power to the injection power required to sustain the end plugs scales as n_c^2/n_p^2. The electron temperature T_e can be increased by auxiliary heating, but it is estimated that to effectively confine a 40-keV central cell plasma with a density of 10^{14} cm^{-3} would require an end plug density of 10^{15} cm^{-3}, which would in turn require neutral beam injection of 600 keV, and peak fields of 17 T [16]. These requirements seemed quite restrictive; in addition, the plasma-surface interactions and materials requirements could be quite severe.

The thermal barrier concept [16] was introduced to ameliorate these requirements. The essence of the idea is to introduce a potential barrier between the end plug and the central cell to more effectively thermally isolate the electrons in these two regions. As a result, each region can be optimized according to its purpose: the central cell plasma can have the high ion energy and density required to produce fusion energy, and the end plug plasma can have a substantially lower ion density but a large ion confining potential to reduce the central cell axial losses. This is achieved by adding rf heating, changing the neutral beam injection angle from perpendicular to the plasma axis to an oblique angle, and adding so-called "ion pumping" of low energy ions trapped in the thermal barrier.

The thermal barrier configuration is made more clear by comparing the axial plasma potential profiles for three end plug configurations shown in Fig. 1. The axial magnetic field profile is shown in Fig. 1a and a schematic of the standard tandem axial potential profile is shown in Fig. 1b. When the end plug beam injection is changed to an oblique angle, the sloshing ion mode of operation results (Fig. 1c). The value of the ion confining potential in this case is equal to that of the conventional tandem. However, the beam-injected mirror-trapped ions (so-called sloshing ions) create an ion density profile that is peaked off the midplane of the plug, thereby causing a potential depression at the midplane; this is advantageous from the standpoint of microstability. It has been shown experimentally that this type of configuration can be created, and that ion fluctuations are low [17].

The thermal barrier axial potential profile is shown in Fig. 1d. The dip in the potential near the midplane is the result of two processes: the formation of a mirror trapped hot electron distribution by means of electron cyclotron resonance heating (ECRH), and the removal of ions from the low potential region by ion pumping. The potential peak is formed by ECRH heating of the electrons in this region. The ion confining potential can be made quite large while the central cell density is greater than the end plug density because of the low passing ion density in the barrier region.

The thermal barrier configuration has also been recently verified experimentally [18,19]; *axial losses of ions can be reduced to nearly* zero. Under these conditions, the end plug plasma is quite microstable because of the shape of the axial ion density profile in the plug (as discussed above) and the central cell ions that pass into the plug region [20]. Control of the neutral pressure in these experiments was shown to be very important, both to minimize charge-exchange losses and to minimize the cold plasma that can fill in the thermal barrier potential region [21]. The edge plasma plays a very important role of shielding the core plasma from neutrals, particularly in the regions where the plasma flux tube is thin.

Several refinements of the thermal barrier concept have recently been made. Again, these were motivated by better understanding of the relevant physics issues and by improved reactor designs. Perhaps one of the most important issues is the control of radial transport. In a tandem mirror with *minimum*-B end plugs, the ions can be transported radially in the central cell by resonant neoclassical transport. As a plasma ion moves from the central cell to the end plug, it passes through a transition region where the magnetic field has a quadrupole component due to the nonaxisymmetric nature of the end plug magnets. As a result, the ion undergoes a radial displacement ΔR at each end of its axial bounce motion. The major component of this displacement and its direction is proportional to cos 2ψ, where ψ is its azimuthal angle. Therefore, if one end plug magnet set is rotated 90^0 with respect to the other end, the radial displacements cancel. However, this cancellation is not complete if an azimuthal drift $\Delta\psi$ is present as a result of radial electric fields in the central cell. Therefore, the causes for resonant neoclassical transport are nonaxisymmetric magnetic fields and azimuthal drifts due to radial electric fields. Detailed explanations of resonant transport are included in Ref. 22.

Several methods of radial transport control have been indentified. Because one major drive is the shape of the magnetic field, it is desirable to terminate the central cell plasma with an axisymmetric magnet that "throttles" the flow of ions passing into the transition regions. This flow of passsing ions is also important for stabilizing trapped particle modes [23], which are similar to those found in tokamaks. An axisymmetic design is incorporated into most current tandem mirror designs, including MFTF-B. Errors in the end plug field due to misalignment can also cause radial transport. This neccesitates careful alignment during construction, often with electron beams, and the addition of "trim" coils for fine adjustment after installation.

The drive for radial transport is also reduced, by controlling the radial potential profile (and therefore the radial electric field) and hence the azimuthal drift. Reducing the radial fields has the added benefit of reducing the rotational drive for instablilites. This radial field profile is determined by the electron losses along field lines to the ends of the machine. If a negative bias is applied to the end wall, the potential in the central cell will decrease to offset this change. In practice, this bias must be a function of radius, so segmented plates are used. This technique has been demonstrated qualitatively in current experiments [24].

Another improvement is the use of drift pumping to remove ions in the thermal barrier regions. Neutral beams--which remove ions by charge exchange--injected nearly parallel to the axis of the machine are the more common method. Drift pumping consists of a field supplied by an external coil that is resonant with a multiple of the bounce or drift frequency of the ions, resulting in a radial displacement. The cumulative result is that the ion eventually leaves the plasma. This technique is attractive because it is selective: it does not pump the sloshing ions, which are not resonant. It is also effective for removing impurities.

The linear geometry of tandem mirrors also makes it possible to directly generate electrical power from any residual axial plasma losses. The conversion efficiency of these devices is usually about 50%. In the original designs, these converters were very large because they depended on the one-dimensional expansion of the plasma fan and subsequent deceleration through a series of grids. Current designs are much more compact because of the use of recircularizing coils to expand the plasma in two dimensions. Gridless converters can be used because the plasma separates the charge carriers: electrons are collected in the core, and ions are collected at the edge.

3. THE THERMAL BARRIER IN MFTF-B

The previous section dealt with the plasma physics issues of a tandem mirror machine in a general way. Next we turn to the specific environment of MFTF-B and how its design addresses these issues. The physics goals of MFTF-B include confinement of reactor-grade central cell plasmas with ion temperatures up to 15 keV, demonstration of high β (the ratio of the plasma pressure to the magnetic field pressure) plasmas approaching 20%, attaining a plasma density-energy confinement time product $n\tau_E$ of approximately 0.6×10^{13} cm^{-3} s, and obtaining a DT equivalent Q of approximately 0.4. These goals represent a significant step toward reactor-type parameters.

In addition, just as reactor designs have motivated the evolution of mirror machine physics, they have also placed requirements on engineering technologies. For this reason, another important function of MFTF-B is to gain experience with some plasma technologies that are relevant to reactors. The design and operation of superconducting magnets with large cryogenic systems will be demonstrated in MFTF-B. Another goal is to address the issues of long pulse operation. The 30-s plasma duration of MFTF-B puts new technological requirements on all of the heating systems: neutral beam injectors, ECRH, and ion-cyclotron resonance heating (ICRH). Nearly steady-state plasma-surface interactions can also be investigated.

Another requirement is a flexible MFTF-B design. As with any large project that requires lead time for construction, modifications may be necessary because of discoveries from current experiments. To date, the modular design of MFTF-B has been used to great advantage to make any necessary changes. In fact, the engineering designs have evolved with relative ease in response to the mirror physics program. The first configuration was a single minimum-B mirror, followed by a tandem mirror with a thermal barrier, and then the addition of a axisymmetric cell for control of radial transport. Even the most recent improvements such as potential control can be integrated easily into the existing design.

The thermal barrier mode for MFTF-B based on the most recent Mirror Advanced Reactor Study (MARS) reactor design is shown in Fig. 2; the steady-state profiles of magnetic field, plasma potential, and density are presented. Such a plasma is created in two steps: a 0.5-s startup sequence followed by 30-s steady-state operation. The central cell is designed to have an electron temperature of 9 keV and an ion temperature of 15 keV. The central cell ion confining potential is about 30 kV. The high magnetic field region in the axicell decreases resonant radial transport and "throttles" the central cell passing particles to allow operation in a regime where trapped particle modes are minimized, as discussed in the previous section. The yin-yang cell provides MHD stability for the system. The desired hot electron distribution (with energies up to 500 keV) is supplied by ECRH injection at three frequencies in the end plug region. Pumping is supplied both by neutral beams in the end region and drift pumping in the transition region.

The vacuum vessel and magnetic field coils for MFTF-B are shown in Fig. 3. Note that the overall length of the vessel is about 64 m. The large cylindrical structures on the outside of the machine are input beamlines and beam dumps for neutral beam injectors. Nearly all of the pumping both in the beamlines and in the plasma vessel is by means of liquid helium cooled cryopanels. A liquid nitrogen guard jacket surrounds each cryopanel and the magnet cases. The magnet system consists of 24 superconducting Nb-Ti coils and two high field Nb_3Sn high field insert coils to provide the 12-T field for the axicell region. Also shown in the figure are the trim coils used in the transition region.

Figure 4 depicts the locations of the neutral beam, ECRH, and ICRH heating systems. Each end plug has three quasi-optical ECRH systems. The 56-GHz systems provide 450 kW at a harmonic of the ECRH resonance to provide a mirror-trapped hot electron distribution. The 28- and 35-GHz systems provide 300 kW near the fundamental ECRH resonance to develop the potential peak. Two frequencies are required because of the β depression by the plasma in this region. These systems are capable of delivering 30-s pulses.

The ICRH transmitters are located off the midplane of the central cell and provide up to 1 MW of power in the frequency range from 6 to 20 MHz in 0.25-MHz steps. A 40% coupling efficiency to the plasma is expected during the steady-state conditions. These transmitters can be operated at this power level for 30 s.

The neutral beams are divided into two classes, 0.5-s beams for startup and 30-s beams for sustaining steady-state operation. The 80-kV startup beams are shown in Fig. 4. There are 10 in the central cell, 1 in each axicell, and 2 in each yin-yang to establish the sloshing ion population. Each beam is designed to provide 50 A of neutral current at the plasma target; the species mix is expected to be 60/20/20% for full/half/third energy components. These beams will have gettered arc chambers to minimize impurity influx. The steady-state 30-s beams are designed to provide 10 A of the full-energy 80-kV component on the plasma target; two each are located in the axicell, the yin-yang or sloshing ion positions, and in the end fans as high energy pump beams (HEPB). Magnetic separation is used to decrease the current of lower energy species to very low levels to minimize barrier filling. In addition, the impurities are reduced to very low levels; this is discussed in more detail in a later section.

Also shown in Fig. 4 are the off-axis 40-kV beams (labeled P2B2) that had been proposed for ion pumping in the transition region. Recent analysis has determined that these beams must pass very close to magnet structures. Beam scrapeoff introduces a source of cold gas. Baffling the beams is difficult and also reduces the beam current. For these reasons, drift pumping of ions has replaced these beams; the physics of the process is described in Ref. 25. Tests of drift pumping will be carried out on TMX-U. Drift pumping is also incorporated into recent MARS reactor designs [8]. In addition, drift pumping has other advantages that are discussed in Sec. 4.2.

4. PLASMA-SURFACE INTERACTIONS IN MFTF-B

In a general sense, the plasma conditions for the MFTF-B central cell are quite similar to other confinement geometries. A dense plasma is confined and heated by auxiliary methods such as ICRH and neutral beams to obtain nearly reactor-like conditions. We might expect that the similarities in these plasmas would in turn lead to similar plasma-surface interactions. However, this is not the case. This is because even though the core plasmas are similar, the edge plasma in a tandem mirror can be quite different (than toroidal plasmas, for example). In addition, the tandem mirror has an extra region that contains both the thermal barrier region and the end wall. Briefly, the tandem mirror allows the possibility of controlling the edge plasma by means of fueling and transport in this region. This relaxes the severity of the plasma-surface interactions, particularly in the fusion-producing central cell region. The plasma lost to the end regions can be controlled so that it is well isolated from the wall. The control of neutrals and impurities is especially important in the thermal barrier region.

The discussion of the relevant plasma-surface interactions can be divided naturally based on the important regions of the machine: interactions at radial surfaces, processes in the thermal-barrier-forming regions, and interactions at the end walls. Impurity generation can be important in all three regions.

4.1 Plasma-Surface Interactions at Radial Surfaces

The linear geometry of a tandem mirror machine allows another degree of freedom for controlling plasma-surface interactions at radial surfaces: axial confinement. In this context, a mirror machine is a "natural" divertor. That is, a region near the plasma edge is formed that has a much shorter axial confinement time than the core of the plasma. In this way, most of the losses of energetic particles flow to the end wall rather than the radial wall. In addition, cold gas and impurities will not have time to penetrate very far before they are lost out of the machine axially. This means that most of the surface interactions will be with neutral atoms, photons, and neutrons.

There is an energy cost to support the edge plasma because as the particles are transported axially they can cause power losses by charge exchange, ionization, and other processes such as radiation. In a reactor, part of this energy could be recovered in the direct converter. In current devices, it puts requirements on the cold gas influx into the system from sources such as neutral beams and on the reduction of reflux from the plasma wall. In the central cell the plasma is quite dense and the corresponding neutral attenuation is large. The thermal barrier region is more sensitive, and is discussed in a subsequent section.

Control of the plasma radius has been demonstrated experimentally on several mirror machines. The single-cell mirror 2XIIB experiment showed that the plasma boundry was determined by the balance of neutral beam fueling and charge-exchange losses on background gas at the plasma edge [26]. In this way, the plasma was not in direct contact with the radial walls. In a conventional tandem mirror such as TMX, each end plug plasma is similar to the single mirror of 2XIIB. In turn, the central cell plasma radius is controlled by the end plug radius because the end plug is responsible for establishing the potential and, hence, axial confinement. In the TMX experiment, the flux tube containing the end plug plasma could be controlled so that it was less than the radius of any physical limiters in the central cell. It was found that the plasma density could be reduced to a very low value near a central cell radial limiter. The central cell plasma radius could also be changed by varying the size of the flux tube that was confined by the end plug plasma [27].

The same type of radial control is possible in a thermal barrier end plug. The radial extent of the barrier is determined by several processes, including filling in by cold ions and electrons, the spatially dependent pumping provided by the neutral beams, and the spatially dependent absorption profile of the ECRH power. For the most part, these processes favor a barrier forming in the core, with a lower confinement time at the edge. Results from TMX-U indicate that this configuration can be established. Under certain conditions, the end loss current is greater in the outside region of the plasma, while the core has virtually no axial losses. A second signature of the influence of the edge plasma in these experiments is the observation of a pressure rise near the end wall during plasma operation [28]. This indicates that plasma is being transported to the end wall by the edge plasma.

Yet another type of radial control is possible based on the control of radial transport in the plasma by biasing the end wall as discussed in Sec. 2. If a region near the edge of the plasma is not biased, then the radial electric field will exist, which can drive resonant transport. In this way, the particles at a certain radius experience radial transport into the edge plasma and cannot support the core plasma; this defines the plasma edge. This technique has the advantage that the plasma radius can be varied without changing any other parameters. Details of the plasma radius control for MFTF-B and MARS are presented in Ref. 29.

The edge plasma operation discussed above will only be efficient if its power requirements are reasonable, that is, if impurity generation and reflux are minimized. In addition, the machine will have to be cleaned initially to obtain optimum operation. Plasma wall conditioning techniques will be required. MFTF-B will contain a plasma wall to shield the plasma from any direct path to a cold surface such as a cryopanel or magnet case. Several methods have been used to condition the walls of mirror machines, and a combination of all of them will be used on MFTF-B. These include: (1) cleaning by repetitive plasma shots, (2) glow discharge cleaning (GDC), and (3) titanium gettering.

The major disadvantage of the first technique in current machines is the low duty cycle. Because 30-s neutral beam operation is possible on MFTF-B, it should be more useful. The second technique has been used successfully on TMX-U [30], essentially replacing method (1) on this machine. On MFTF-B, GDC may be somewhat more complicated, as the magnetic field must be off and the pumping capacity of the cryopumping system may be exceeded during extended operation at the required pressures. This requires operation of GDC without the cryopanels and with auxiliary pumping. In addition, specialized coatings on the cryopanel surfaces may be degraded by the GDC; although experiments [31] have shown that electrical isolation of the cryopanels will minimize this damage. Titanium gettering will also be used. Experiments are underway on operating experiments to determine the required frequency and coverage of gettering [32,33].

Another conditioning technique that is particularly attractive for MFTF-B is made possible by the steady-state magnetic field and the 30-s pulse length of the ECRH and ICRH systems. Experiments have shown that a tandem mirror plasma can be sustained with ICRH alone [34]; this would enable the formation of a confined plasma at fairly low pressures that would condition only the plasma walls. Combinations of ECRH and ICRH have been successful in conditioning RFC-XX [35]. If effective in MFTF-B, it would bypass most of the complications associated with GDC.

4.2 Plasma-Surface Interactions in the Thermal Barrier

The parameters of the thermal barrier region can be limited by the charge exchange of hot ions, the filling in of the barrier by trapping of cold neutrals, and the filling in of the positive potential peak by cold electrons. In addition, the plasma flux tube is thinner (fan-shaped) and the density is less in this region, so neutral shielding by the core of the plasma is less than in the central cell This means that the combination of the shielding and particle removal by the edge plasma, the pumping in this region, and the control of cold gas sources from neutral beams and wall reflux must be sufficient to prevent the loss processes from becoming important.

Calculations for MFTF-B have been carried out to ensure that the loss processes can be controlled. Filling in of the thermal barrier region by trapping of cold neutrals has been found to be the most important limiting process. This establishes a requirement of maintaining the on-axis neutral density below 10^7 to 10^8 cm^{-3} in this region. A gas penetration code [36] is then used along with the expected plasma parameters to calculate the neutral attenuation by the plasma, which determines the neutral density at the edge plasma. The model indicates that the edge pressure must be in the 10^{-7} to 10^{-6} Torr range. This pressure must be consistent with the supplied pumping speed of the system and the sources. Calculations indicate that the requirements can be met, as long as wall reflux does not exceed unity by a large amount and gas sources from neutral beams are well controlled.

This model has also been compared with experimental results from TMX-U [21] and is in qualitative agreement. The importance of the control of neutral gas is demonstrated in Fig. 5 [21], in which the pressure in the end plug and the ion end losses are shown as a function of time for two cases. In the left half of the figure, the neutral beam gas and wall reflux are not carefully controlled, and the thermal barrier plugging (reduction of end losses) is lost when the end plug pressure rises. In the right half of the figure, extensive baffling of the cold gas and reduction of wall reflux has resulted in a lower end plug pressure and a longer plugging of the axial losses.

These same measures have been incorporated into the MFTF-B vacuum system. Neutral beam injectors, when possible, are connected to the vessel through a beamline with extensive differential pumping. When it is necessary to locate the beam closer to the plasma, the beam line is incorporated into the machine by installing baffles and pumping. Beam dumps are located in separate tanks across from the beam, or in large pumping chambers incorporated into the vessel. A schematic of an external beamline and an internal beam dump is shown in Fig. 6. Reflux is controlled by wall conditioning techniques, especially gettering.

Impurities can also degrade the thermal barrier because they are efficiently trapped in the potential minimum. Cold impurities are expected to be shielded from the barrier region by the edge plasma. However, impurities present in neutral beams that are used to fuel and pump the thermal barrier can penetrate into the core. Figure 7 shows impurity emissions from several oxygen, nitrogen, and carbon lines during a plasma shot on TMX-U. Note that the nitrogen and oxygen emissions decrease rapidly when the neutral beam is turned off, indicating that the beam is a source of these impurities. Estimates indicate that about 1% of the beam current in normal injectors can be oxygen [37]. Because these impurities can be so detrimental, two steps have been taken in MFTF-B beam sources. In the 0.5-s beams, the arc chambers are gettered; tests have shown that this can reduce the impurity current to less than 0.1%. For the 30-s sources, magnetic separation is incorporated into the design, a schematic of such a source is shown in Fig. 8. The expected impurity current is in the range of 0.001 to 0.0001%; these sources are currently being tested. Models have shown than this reduction should be sufficient for thermal barrier operation [38].

Finally, it should be noted that other means of pumping the thermal barrier region, such as drift pumping in MFTF-B, should also be advantageous from the standpoint of plasma-surface interactions. This method is not expected to produce any neutral gas or impurity influx. Ions are moved radially to the edge plasma, where they are transported to the end fan regions and are pumped. This is in contrast to neutral beam pumping, where ions are charge exchanged into neutrals that are lost in the pumping region. In addition, it might be possible to selectively pump impurities from the system.

4.3 Plasma-Surface Interactions at the End Walls

In early mirror machines, a target plasma was injected along field lines by a plasma gun. This created a plasma between the end wall and the magnetic mirror which could cause large power losses [39]. This problem was minimized by the use of a pulsed plasma gun and pulsed magnetic fields, thereby breaking the connection to the end wall. In modern tandem mirrors, ECRH is used to initiate the plasma [40] for thermal barrier operation, and this mode of startup is also planned for MFTF-B. ECRH startup also removes one source of impurities because some plasma guns injected titanium [41] directly into the plasma.

Control of the plasma density in the neighborhood of the end wall is important to minimize power losses. A fraction of hot ions is not confined and is lost to the end wall; the density of these ions can be controlled by expanding the plasma flux tube by decreasing the magnetic field from the outside mirror point to the end wall. Explicitly, $j_w = (B_m/B_w)\, j_m$ where j is the ion current density and B is the magnetic field; the subscripts w and m refer to the wall and the mirror point, respectively. The reduction of density was experimentally verified on TMX, where the magnetic field ratio was about 200 [42]. On MFTF-B, the magnetic field ratio is equal to 60.

A second source of power loss could be caused by the cold ions produced from recycling at the end wall. The cold neutrals produced by interactions with the end wall must be pumped before they ionize and accumulate in the end region. The plasma density control discussed above plays a role in this process, as the mean time between ionizations will be longer at low density, resulting in a higher pumping probability. A model has been computed for MFTF-B [43] that indicates that gas accumulation should not be a problem with the available pumping.

The potential near the end wall can also be important. It has been shown experimentally that the electron temperature near the end wall can be small, which leads to a small sheath potential, reducing the probability of unipolar arcs [27]. Secondary electron emission at the endwalls was once thought to be a major problem in mirror machines, limiting the electron temperature by allowing hot electrons to escape [39]. When space charge limiting effects were considered, as in the model discussed above [43], it was found that only modest increases in the end loss power would occur. In the case of MFTF-B, an enhancement of only 40% is predicted for a particle reflux coefficient of unity even if the electron temperature near the end wall is equal to the central cell temperature. The actual temperature in the region near the end wall is expected to be much less than this value, so the effect of secondaries is expected to be even smaller.

Impurity generation in this region is not anticipated to be a problem, as ions must penetrate the large axial potential to influence the rest of the plasma region. Radiation losses should be small for impurities in this area because the electron density and temperature are low.

5. SUMMARY

MFTF-B, a large tandem mirror machine under construction at LLNL, represents the next generation of these devices. It is designed to confine reactor-like plasmas. It will also address certain technological issues such as operation of superconducting magnet systems and long pulse (30 s) operation. Plasma-surface interactions at radial surfaces can be minimized due to the control of the edge plasma confinement which can be lost axially. Gas and impurity sources must be carefully controlled in the thermal barrier region, requiring gas control in the neutral beams and also impurity control by gettering and magnetic separation. Wall interactions at the end of the machine can be minimized by expanding the plasma flux tube, and controlling gas recycling. Wall conditioning techniques will be employed that are similar to other machines; the steady state heating systems will also be used.

In summary, present experiments along with current models indicate that plasma-surface interactions are expected to be controllable in large devices such as MFTF-B. Current experiments will be used to optimize these methods of control, particularly in the thermal barrier region. Several experiments are examining novel techniques, including metal vapor jets to control neutral beam gas, and operation with high temperature plasma walls [4]. Diagnostic techniques are also becoming much more sophisticated, including laser fluorescence measurements of the neutral density [44]. Most importantly, most of the methods used to control plasma-surface interactions in large machines such as MFTF-B are also relevant to current reactor designs.

REFERENCES

[1] Simonen, T. C., D. E. Baldwin, S. L. Allen, et al., "TMX Tandem Mirror Experiments and Thermal-Barrier Theoretical Studies," in Proc. 9th Intern. Conf. Plasma Physics and Controlled Nuclear Fusion Research, held in Baltimore, MD, 1982 (IAEA, Vienna, 1983), vol. 1, p. 519.

[2] Hershkowitz, N., R. A. Breun, D. Brouchous, et al., "Recent Experiments in the Phaedrus Tandem Mirror," in Proc. 9th Intern. Conf. Plasma Physics and Controlled Nuclear Fusion Research, held in Baltimore, MD (1982), IAEA, Vienna, 1983, vol. 1, p. 553.

[3] Inutake, M., K. Ishii, A. Itakura, et al., "Studies of Improvement of Plasma Confinement in Axisymmetrized Tandem Mirror," in Proc. 9th Intern. Conf. Plasma Physics and Controlled Nuclear Fusion Research, held in Baltimore, MD, (1982), IAEA, Vienna, 1983, vol. 1, p. 545.

[4] Dimov, G. I. and G. V. Roslyakov (1981), "A Trap With Ambipolar Plugs," (Institute of Nuclear Physics, Novosibirsk, USSR, Preprint 80-1520), published by Lawrence Livermore National Laboratory, Livermore, CA, UCRL-TRANS-11670.

[5] Kesner, J., R. S. Post, B. D. McVey, and D. K. Smith (1982a), "A Tandem Mirror with Axisymmetric Central-Cell Ion Confinement," Nucl. Fusion 22, 549-560.

[6] Hsu, W. L., "Review of Plasma Wall Interaction Experiments on TMX and TMX-U," in Proc. 6th Intl. Conf. on Plasma-Surface Interactions in Controlled Fusion Devices, Nagoya, Japan (1984). To be published in the J. of Nucl. Instr. and Mater.

[7] Thomassen, K., B. G. Logan, J. N. Doggett, and F. H. Coensgen, "A DT-Burning Upgrade to MFTF-B", in Proc. 6th Intl. Conf. on Plasma-Surface Interactions in Controlled Fusion Devices, Nagoya, Japan (1984).

[8] Logan, B. G. et al., MARS Final Report, Lawrence Livermore National Laboratory, Livermore, CA, UCRL-53480 (to be published 1984).

[9] Damm, C. C., J. H. Foote, A. H. Futch, A. L. Gardner, and R. F. Post, Phys. Rev. Lett. 13, 464 (1964).

[10] Moir, R. W. and R. F. Post, Nucl. Fusion 9, 253 (1969).

[11] Post, R. F., Proc. Intl. Conf. Plasma Confined in Open-Ended Geometry (Gatlinburg, TN, 1967), p. 309; also published as Oak Ridge National Laboratory Report CONF-671127.

[12] Coensgen, F. H., W. F. Cummins, B. G. Logan, A. W. Molvik, W. E. Nexsen, T. C. Simonen, B. W. Stallard, and W. C. Turner, Proc. 7th Eur. Conf. Cont. Fusion Plasma Phys., (1975) Vol. II, p. 167.

[13] Moir, R. W., Lawrence Livermore National Laboratory Report UCID-17644 (1978).

[14] Correll, D. L. et al., Nucl. Fusion 22, 223 (1982).

[15] Casper, T. A. and G. R. Smith, Phys. Rev. Lett. 48 (1982) 1015.

[16] Baldwin, D. E. and B. G. Logan, Phys. Rev. Lett. 43, 1318 (1979).

[17] Simonen, T. C. et al., Phys. Rev. Lett. 50, 1668 (1983).

[18] Grubb, D. P., S. L. Allen, J. D. Barter, et al., "Thermal Barrier Production and Identification in a Tandem Mirror," submitted to Phys. Rev. Lett.; Lawrence Livermore National Laboratory, Livermore, CA, UCRL-90536.

[19] Simonen, T. C., S. L. Allen, T. A. Casper, et al., "TMX-U Experimental Results," Course/Workshop on Mirror-Based Approaches to Magnetic Fusion, Varenna, Italy, Sept. 7-17, 1983; published by Lawrence Livermore National Laboratory, Livermore, CA, UCRL-89286 (1983).

[20] Casper, T. A., L. V. Berzins, R. F. Ellis, R. A. James, and C. Lasnier, "Microstability of TMX-U During Initial Thermal Barrier Operation," Intl. Conf. on Plasma Physics, Lausanne, Switzerland (1984); Lawrence Livermore National Laboratory, Livermore, CA, UCRL-90451.

[21] Turner, W. C., W. E. Nexsen, S. L. Allen, et al., "Gas Pressure in the End Plug Regions of the TMX-U Thermal Barrier Experiment," submitted to the Journal of Vacuum Science and Technology (1983); Lawrence Livermore National Laboratory, Livermore, CA, UCRL-89938.

[22] Mirin, A. A., S. P. Auerbach, R. H. Cohen, J. M. Gilmore, L. D. Pearlstein, and M. E. Rensink, Nucl. Fusion 23, 703 (1983). See also D. E. Baldwin and B. G. Logan (Eds.), "Physics Basis for an Axicell Design for the End Plugs of MFTF-B," Lawrence Livermore National Laboratory, Livermore, CA, UCID-19359 (1982).

[23] Pearlstein, L. D., D. E. Baldwin, R. H. Cohen, T. K. Fowler, and B. G. Logan, "Stabilization of Tandem-Mirror Trapped-Particle Modes by Incomplete Cancellation of Trapped-Particle Drifts," presented at 1982 Sherwood Meeeting, Annual Controlled Fusion Theory Conference, Santa Fe, NM, April 25-28, 1982.

[24] Hooper, E. B. Jr., D. E. Baldwin, T. K. Fowler, R. J. Kane, and W. C. Turner, "Radial Transport Reduction in Tandem Mirrors Using End Wall Boundary Conditions," submitted to Physics of Fluids (1984); Lawrence Livermore National Laboratory, Livermore, CA, UCRL-90639.

[25] Chen, Y-J., D. E. Baldwin, and T. Q. Hua, "Analytic Model and Simulations of RF Drift Pumping of Thermal Barriers," Bull. Amer. Phys. Soc. 28 (1983) p. 1195.

[26] Stallard, B. W., F. H. Coensgen, W. F. Cummins, et al., "Plasma Wall Charge Exchange Interactions in the 2XIIB Magnetic Mirror Experiment," in Proc. International Symposium on Plasma Wall Interaction, Jülich, Federal Republic of Germany (1976), Pergamon Press, p. 63.

[27] Drake, R. P., "Control of Plasma/Wall Interactions in Tandem Mirrors," Nuclear Technology Fusion 3 (1983) 405.

[28] Simonen, T. C., S. L. Allen, W. L. Bauer, and W. Hsu, A Model for the Edge Plasma of a Tandem Mirror, report in preparation at Lawrence Livermore National Laboratory, Livermore, CA.

[29] Najmabadi, F. and R. W. Conn, "Radius Control System for Tandem Mirrors," submitted to Nuclear Technology/Fusion (1984).

[30] Allen, S. L., C. Clower, R. P. Drake, E. B. Jooper, Jr., A. L. Hunt, R. Munger, R. J. Bastasz, W. Bauer, and W. L. Hsu, "Initial Wall Conditioning for the TMX-U Fusion Experiment, J. Vac. Sci. Technol. A 1(2) (1983) 916.

[31] Osher, J. E., G. D. Porter, L. E. Valby, Glow Discharge Cleaning Tests of MFTF-B Cryopanel Components, Lawrence Livermore National Laboratory, Livermore, CA, Quarterly Jan.-May, 1981, UCRL-50051-81-1 (1981).

[32] Edmonds, P. H., P. Mioduszewski, J. E. Simpkins, A. J. Wooten, Journal Vac. Sci. and Tech. 20 (1982) 1317.

[33] Allen, S. L., C. A. Clower, and W. C. Turner, "The Influence of Vacuum and Wall Conditions on Plasma Startup in TMX-U," Bull. Amer. Phys. Soc. 28 (1983) 1114.

[34] Ferron, J. R., R. A. Breun, S. N. Golovato, "Scaling of RF Sustained Tandem Mirror Parameters With Central Cell Heating Power Including a Central Cell Stand-Alone Mode," Bull. Amer. Phys. Soc. 27 (1982) 958.

[35] Garner, D., private communications, May 1984.

[36] Gryczkowski, G. E., Neutral Gas Blanket Theory as Applied to the Reference Theta Pinch Reactor, Ph.D. Thesis, Univ. of Michigan, Dept. of Nuclear Engineering (1979).

[37] Drake, R. P. and H. W. Moos, Nucl. Fus. 19 (1979) 407.

[38] Osher, J. E., D. P. Grubb, and P. Poulsen, "Impurity Accumulation in a Tandem Mirror," Bull. Amer. Phys. Soc. (1983) 1119.

[39] Hall, L. S., Nucl. Fusion 17, 681 (1977).

[40] Stallard, B. W., "ECRH in Tandem Mirror Machines," IEEE Minicourse on RF Heating and Current Drive, San Diego, CA (1983); Lawrence Livermore National Laboratory. Livermore, CA, UCRL-89276.

[41] Allen, S. L., T. L. Yu, T. J. Nash, "Impurity Characteristics of TMX-U," Lawrence Livermore National Laboratory, Livermore, CA, UCID-20026 (1984).

[42] Coakley, P., N. Hershkovitz, and G. D. Porter, "End-Wall Plasma Characteristics in the Tandem Mirror Experiments," Nucl. Fusion 22, 1321 (1982).

[43] Porter, G. D., "Effect of Gas Recycling and Secondary Emission on the Axial Flow in an Open-Ended Device," Nucl. Fusion 22, 1279 (1982).

[44] Muraoka, K., M. Maeda, T. Okada, et al., 6th Intl. Conf. on Plasma Surf. Int. in Cont. Fus. Devices (1984).

FIGURE CAPTIONS

Fig. 1. The operating modes of a tandem mirror help illustrate the thermal barrier configuration. The axial magnetic field profile in the end plug is illustrated in (a). The axial potential profile for the conventional tandem mode is shown in (b). Changing the end plug neutral beams to off-axis injection results in the sloshing ion mode profile in (c). Addition of ECRH and ion pumping is required for the thermal barrier shown in (d).

Fig. 2. The axial profiles of magnetic fields, potential, and density are shown for MFTF-B. The thermal barrier region is in the yin-yang cell.

Fig. 3. The vacuum vessel of MFTF-B with its associated neutral beamlines is shown. The right half of the figure is cut away to show the superconducting magnets.

Fig. 4. The neutral beam and rf heating locations for MFTF-B. The bottom half of the figure indicates the azimuthal angle where the 0.5 s and 30 s neutral beam sources are located.

Fig. 5. The end plug pressure and the axial ion loss as a function of time in TMX-U. In (a), the plugging ceases as the pressure increases. In (b), measures have been taken to reduce the cold gas sources and wall reflux, resulting in a reduced pressure rise and a longer duration of plugging. This illustrates the importance of gas and reflux control in the thermal barrier region.

Fig. 6. Schematic representation of external beamlines and integral beam dumps for MFTF-B. These are important for the reduction of gas, particularly in the thermal barrier region.

Fig. 7. The time histories of carbon, nitrogen, and oxygen ionization states are shown; the neutral beams are turned off at 35 ms. Note that the nitrogen and oxygen emissions decrease at this time.

Fig. 8. Schematic of the pure beam injectors for MFTF-B. These beams provide 10 A of full energy, low impurity current.

(a) 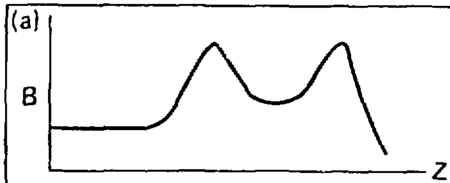	Input power	Potential confinement	End cell ion microstability (source of low energy ions)
(b) Original tandem mode 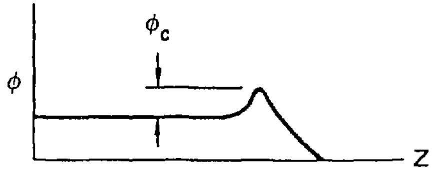	90° beams	$\phi_c = T_e \ln\left(\frac{n_p}{n_c}\right)$	Center cell ion losses
(c) Sloshing ion mode 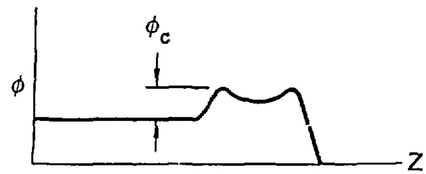	Off axis beams	$\phi_c = T_e \ln\left(\frac{n_p}{n_c}\right)$	Potential trapped ions <u>and</u> central cell ion losses
(d) Thermal barrier mode 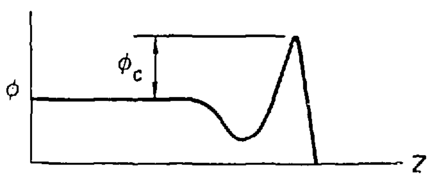	ECRH off axis beams Pump beams	Strong ECRH MFTF-B $\phi = T_{ec}\left\{\frac{\sqrt{\pi}}{4}\left(\frac{n_p}{n_b^*}\right)\left(\frac{n_c}{n_b^*}\right)^{1/2}\right\}^{2/3} - T_{ec}\ln\left(\frac{n_c}{n_b^*}\right)$	Potential trapped ions <u>and</u> passing center cell ions

Allen - Fig. 1

Allen - Fig. 2

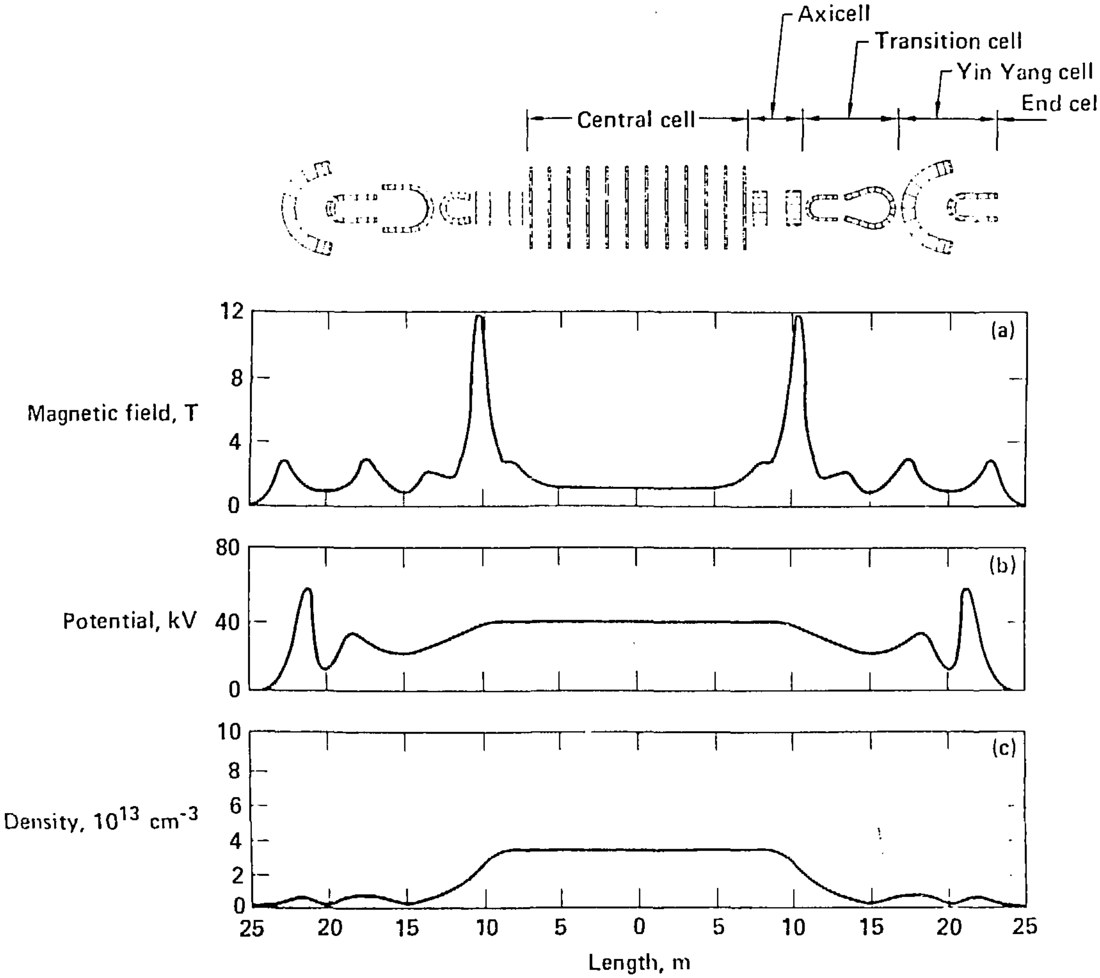
Axicell
Transition cell
Yin Yang cell
End cell
Central cell
Magnetic field, T
Potential, kV
Density, 10^{13} cm^{-3}
(a)
(b)
(c)
Length, m
25 20 15 10 5 0 5 10 15 20 25

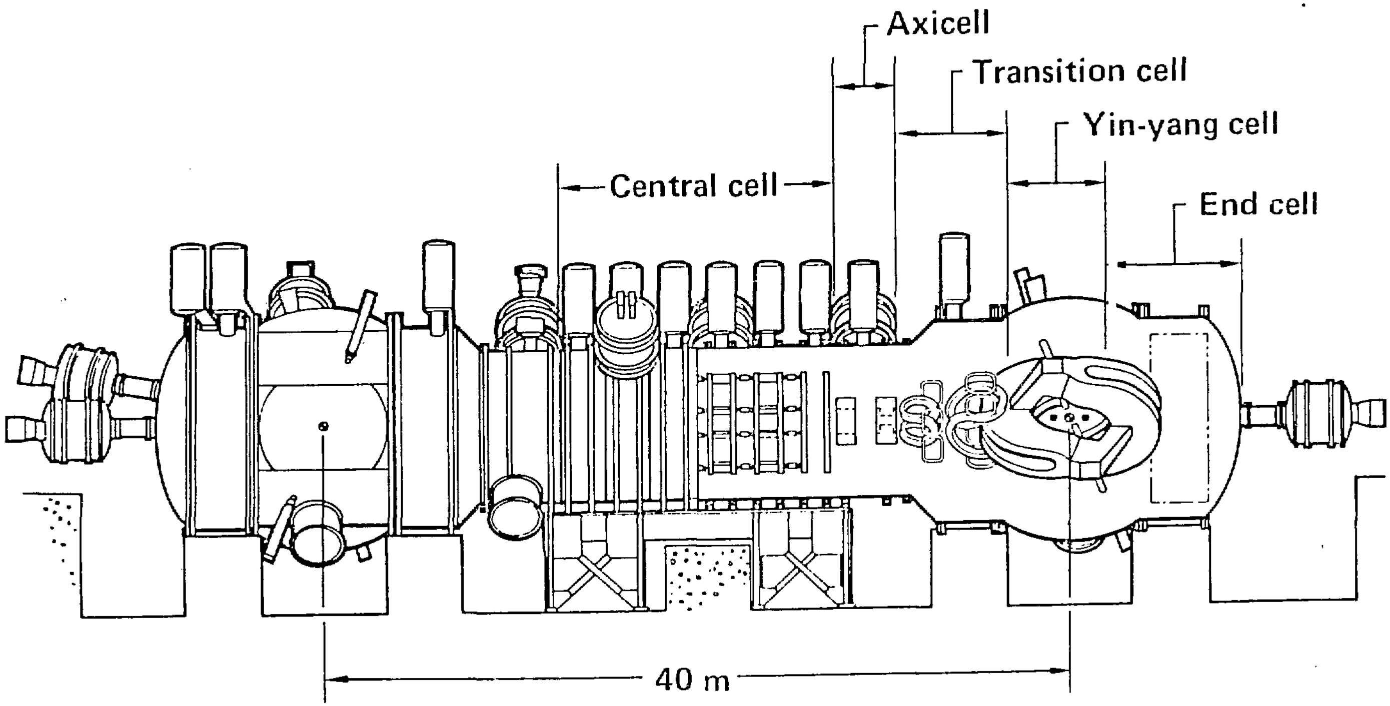
Axicell
Transition cell
Yin-yang cell
Central cell
End cell
40 m

Allen - Fig. 3

Allen - Fig. 4

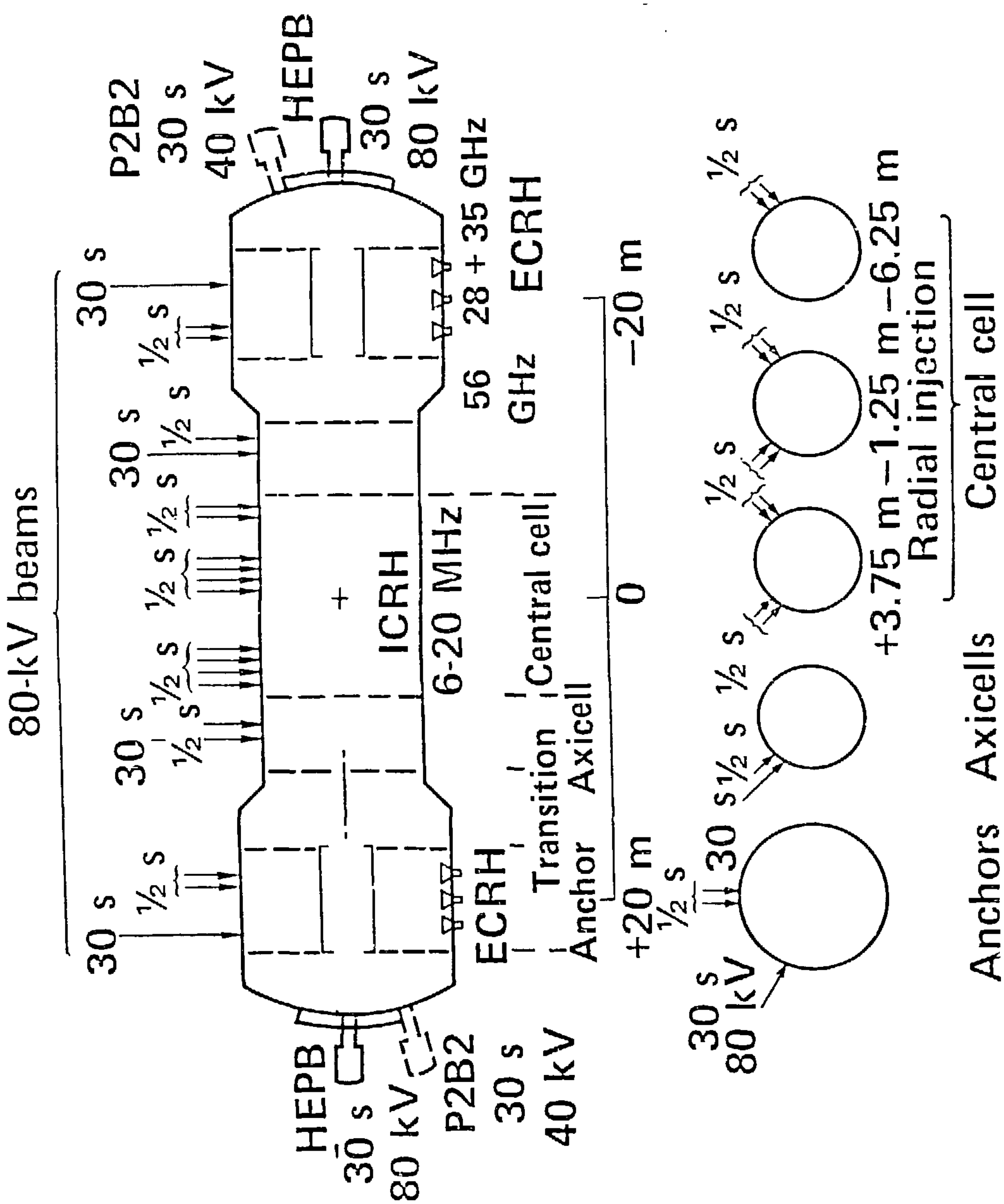
80-kV beams
30 s
½ s
P2B2
30 s
40 kV
HEPB
30 s
80 kV
28 + 35 GHz
ECRH
56 GHz
ICRH
6-20 MHz
Central cell
Transition
Axicell
Anchor
ECRH
+20 m
0
−20 m
+3.75 m −1.25 m −6.25 m
Radial injection
Central cell
Axicells
Anchors

Allen - Fig. 5

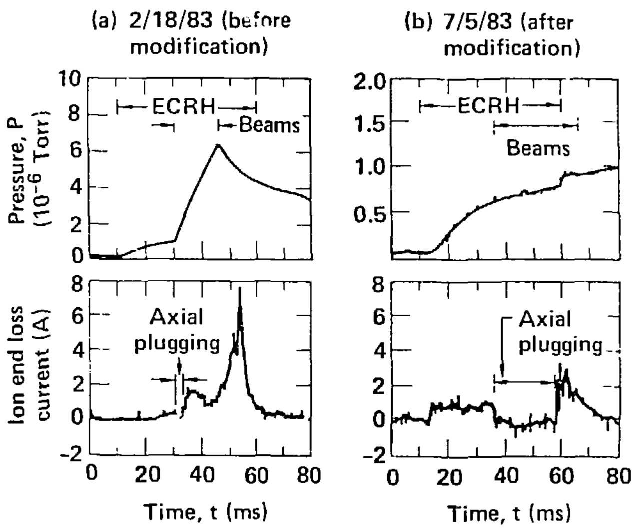
(a) 2/18/83 (before modification)
(b) 7/5/83 (after modification)
Pressure, P (10^{-6} Torr)
ECRH
Beams
Ion end loss current (A)
Axial plugging
Time, t (ms)

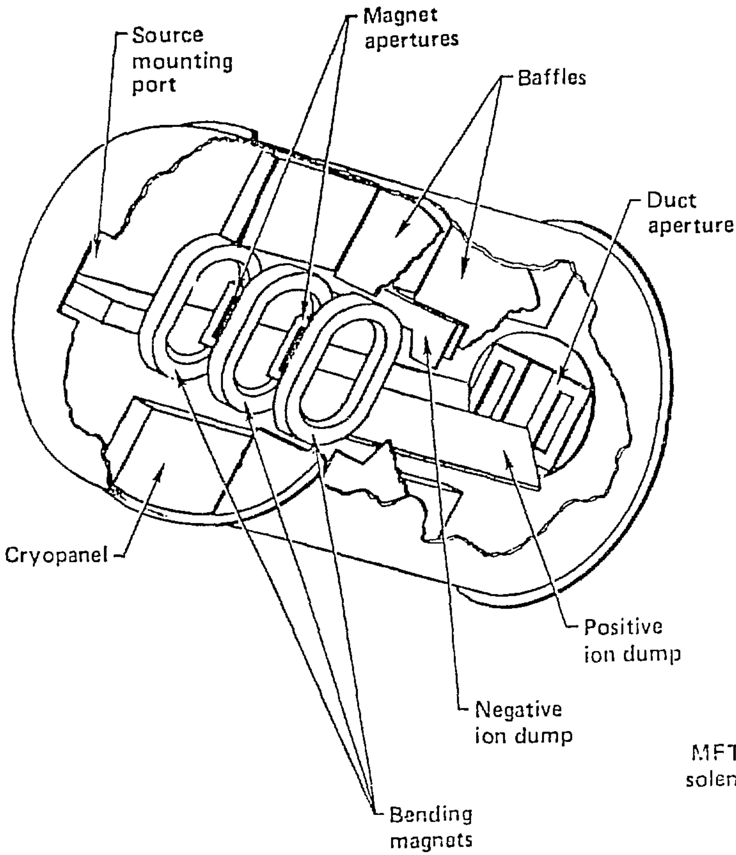

External beam line

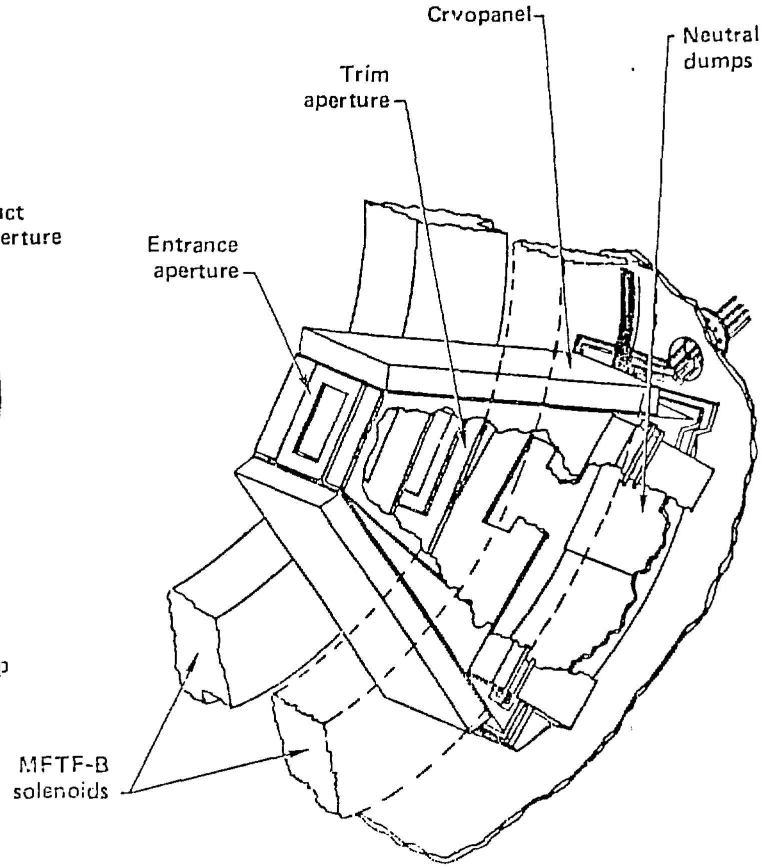

Internal beam dump

Allen - Fig. 6

Allen - Fig. 7

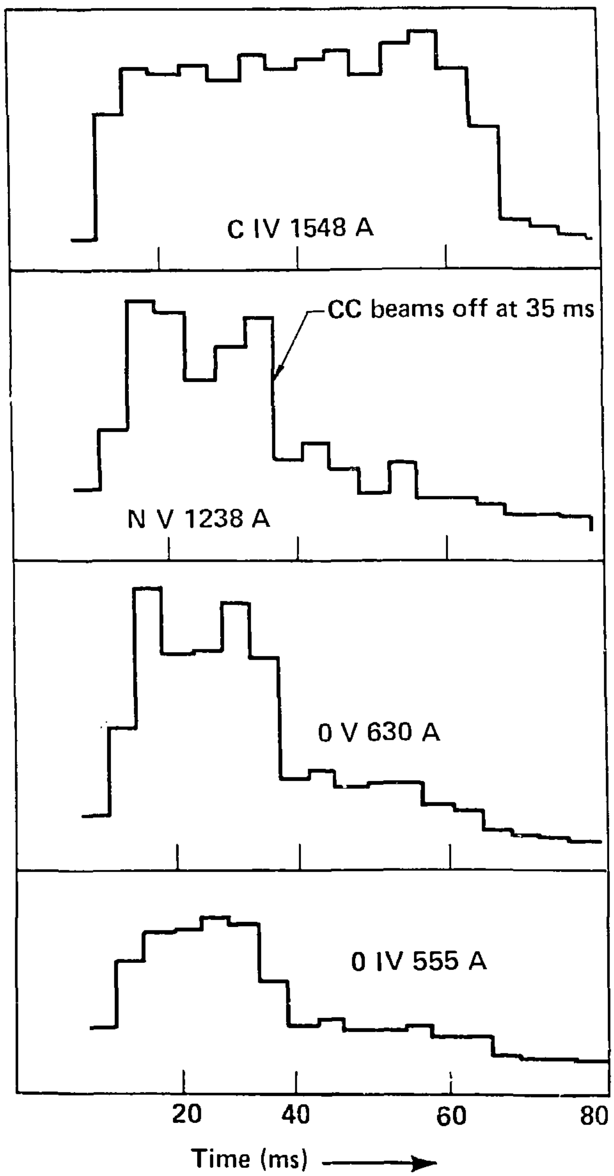
C IV 1548 A
CC beams off at 35 ms
N V 1238 A
0 V 630 A
0 IV 555 A
20
40
60
80
Time (ms)

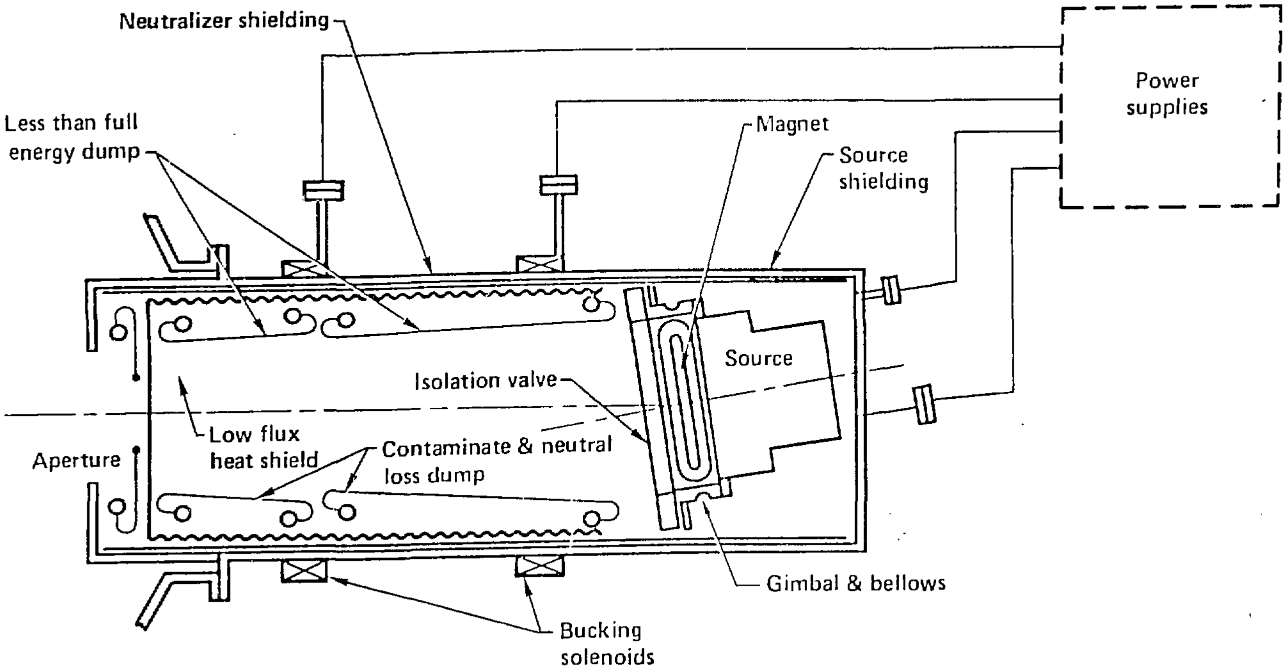
Neutralizer shielding
Power
supplies
Less than full
energy dump
Magnet
Source
shielding
Source
Isolation valve
Low flux
heat shield
Contaminate & neutral
loss dump
Aperture
Gimbal & bellows
Bucking
solenoids

Allen - Fig. 8